

Neuronal Excitability

# $\Delta$ FosB Decreases Excitability of Dorsal Hippocampal CA1 Neurons

** Andrew L. Eagle, Elizabeth S. Williams, Joseph A. Beatty, Charles L. Cox, and Alfred J. Robison**DOI:<http://dx.doi.org/10.1523/ENEURO.0104-18.2018>

Department of Physiology and Neuroscience Program, Michigan State University, East Lansing, Michigan 48824

## Abstract

Both the function of hippocampal neurons and hippocampus-dependent behaviors are dependent on changes in gene expression, but the specific mechanisms that regulate gene expression in hippocampus are not yet fully understood. The stable, activity-dependent transcription factor  $\Delta$ FosB plays a role in various forms of hippocampal-dependent learning and in the structural plasticity of synapses onto CA1 neurons. The authors examined the consequences of viral-mediated overexpression or inhibition of  $\Delta$ FosB on the function of adult mouse hippocampal CA1 neurons using *ex vivo* slice whole-cell physiology. We found that the overexpression of  $\Delta$ FosB decreased the excitability of CA1 pyramidal neurons, while inhibition increased excitability. Interestingly, these manipulations did not affect resting membrane potential or spike frequency adaptation, but  $\Delta$ FosB overexpression reduced hyperpolarization-activated current. Both  $\Delta$ FosB overexpression and inhibition decreased spontaneous excitatory postsynaptic currents, while only  $\Delta$ FosB inhibition affected the AMPA/NMDA ratio, which was mediated by decreased NMDA receptor current, suggesting complex effects on synaptic inputs to CA1 that may be driven by homeostatic cell-autonomous or network-driven adaptations to the changes in CA1 cell excitability. Because  $\Delta$ FosB is induced in hippocampus by drugs of abuse, stress, or antidepressant treatment, these results suggest that  $\Delta$ FosB-driven changes in hippocampal cell excitability may be critical for learning and, in maladaptive states, are key drivers of aberrant hippocampal function in diseases such as addiction and depression.

**Key words:**  $\Delta$ FosB; CA1; excitability; hippocampus; transcription factor

## Significance Statement

Memory consolidation is a key component of adaptive learned behavior, which can be disrupted in psychiatric conditions, and regulated gene expression in hippocampus is critical for learning and memory.  $\Delta$ FosB is a highly stable, activity-dependent transcription factor that regulates hippocampus-dependent memory, yet its specific role in hippocampal neuronal function is unclear. The authors use whole-cell slice electrophysiology to uncover a novel role for  $\Delta$ FosB in regulating neuronal excitability in the CA1 region of hippocampus. These findings suggest that  $\Delta$ FosB-driven changes in gene expression drive the intrinsic excitability of hippocampal CA1 pyramidal neurons, potentially regulating learning, antidepressant responses, and psychiatric diseases such as drug addiction and depression.

## Introduction

Memory consolidation is indispensable to mammalian survival, and disruption of memory underlies numerous aberrant clinical conditions including neurodegenerative

disorders, psychiatric disease, and neurodevelopmental impairments. The formation and retrieval of memories rely on changes in gene expression, and activity-dependent gene transcription in the hippocampus (HPC),

Received March 19, 2018; accepted July 13, 2018; First published July 23, 2018.

The authors declare no competing financial interests.

Author contributions: A.L.E., J.A.B., C.L.C., and A.J.R. designed research; A.L.E., E.S.W., and J.A.B. performed research; A.L.E. and E.S.W. analyzed data; A.L.E., E.S.W., and A.J.R. wrote the paper.

in particular, is necessary for long-term memory consolidation and normal HPC function (Alberini and Kandel, 2014; Eagle et al., 2016). Transcription underlies durable modifications in HPC neuronal physiology, including synaptic and nonsynaptic plasticity (Guzman-Karlsson et al., 2014), and it is well established that pharmacological blockade of transcription impairs long-term plasticity and memory consolidation (Squire and Barondes, 1970; Frey et al., 1996; Lee et al., 2004). Given that this process is important for HPC function and learning, it is critical that we fully delineate the mechanism by which activity-dependent changes in gene transcription drive altered neuronal physiology.

$\Delta$ FosB is a unique activity-dependent transcription factor that is remarkably stable, with a half-life of up to 8 d in the brain (Carle et al., 2007; Ulery-Reynolds et al., 2009; Cates et al., 2014), thereby making it an interesting candidate for regulation of gene transcription in long-lasting processes such as memory consolidation. Hippocampal  $\Delta$ FosB is important for learning and CA1 neuron structural plasticity (Eagle et al., 2015; Corbett et al., 2017).  $\Delta$ FosB is induced specifically in dorsal HPC (dHPC) CA1 pyramidal neurons during spatial learning, and its transcriptional activity in those cells is crucial for multiple HPC-dependent forms of learning and memory. However, the physiologic mechanism by which  $\Delta$ FosB regulates hippocampal neuronal function remains unknown.

$\Delta$ FosB differentially regulates synaptic strength in dopamine D<sub>1</sub> and D<sub>2</sub> receptors expressing medium spiny neurons (MSNs) of the nucleus accumbens (NAc) in a subregion-specific manner (Grueter et al., 2013). These findings suggest that  $\Delta$ FosB induces cell type-specific plasticity in NAc and that this may provide a novel target for the treatment of addiction and depression.  $\Delta$ FosB in prefrontal cortex may also regulate projection-specific cell function, and this may underlie depressive and/or post-traumatic stress disorder phenotypes (Vialou et al., 2014). Because its role in HPC cell function remains unknown, we investigated the role of  $\Delta$ FosB in membrane properties, excitability, and synaptic function in dHPC neurons. We used viral-mediated gene transfer to overexpress  $\Delta$ FosB or silence its transcriptional activity specifically in dorsal CA1 neurons *in vivo* and examined cell properties *ex vivo* using slice whole-cell electrophysiology. We report here that  $\Delta$ FosB reduces neuronal excitability in CA1 neurons of the dHPC.

This work was supported by National Institute of Mental Health Grants R01-MH-111604 (A.J.R.) and R01-MH-085324 (C.L.C.), the Whitehall Foundation (A.J.R.), and the Brain and Behavior Research Foundation NARSAD Young Investigator Award (A.L.E.).

Correspondence should be addressed to Alfred J. Robison, Department of Physiology, Michigan State University, 567 Wilson Road, East Lansing, MI 48824. E-mail: robiso45@msu.edu

DOI: <http://dx.doi.org/10.1523/ENEURO.0104-18.2018>

Copyright © 2018 Eagle et al.

This is an open-access article distributed under the terms of the Creative Commons Attribution 4.0 International license, which permits unrestricted use, distribution and reproduction in any medium provided that the original work is properly attributed.

## Materials and Methods

### Animals

This study followed guidelines described in the *Guide for the Care and Use of Laboratory Animals* (Institute of Laboratory Animal Resources (U.S.), 2011). All animal procedures were performed in accordance with the regulations of the Michigan State University animal care committee. Adult male C57BL/6J mice (<https://www.jax.org/strain/000664>), 7–9 weeks of age, were group housed ( $n = 4$ –5/cage) in a vivarium and kept at 20–23°C under a 12 h light/dark cycle with *ad libitum* access to food and water.

### Viruses and surgery

Mice received viral infusions into the dHPC. Stereotaxic surgery was performed to inject herpes simplex virus (HSV) vectors into bilateral dHPC, as follows: 7° angle; –2.2 mm anteroposterior,  $\pm 2.0$  mm ML, –2.0 and –1.8 mm DV (0.3  $\mu$ l of purified virus was infused at each DV site at a rate of 0.1  $\mu$ l/min). HSV expressing GFP,  $\Delta$ FosB + GFP, or  $\Delta$ JunD + GFP driven by the cytomegalovirus promoter were obtained from the Massachusetts Institute of Technology Viral Core Facility [now moved to Massachusetts General Hospital (<https://researchcores.partners.org/mvvc/about>)]. The approximate titer for all viruses used was  $\sim 1.0 \times 10^9$  virions/ml.

### Slice preparation

All solutions were bubbled with 95% O<sub>2</sub>–5% CO<sub>2</sub> throughout the procedure. Mice were anesthetized with isoflurane and transcardially perfused with sucrose artificial CSF (aCSF; in mM: 234 sucrose, 2.5 KCl, 1.25 NaH<sub>2</sub>PO<sub>4</sub>, 10 MgSO<sub>4</sub>, 0.5 CaCl<sub>2</sub>, 26 NaHCO<sub>3</sub>, and 11 glucose). Brains were rapidly removed, blocked, and placed in cold sucrose aCSF. Coronal sections (250  $\mu$ m) containing dHPC were cut on a vibratome (Leica) and transferred to an incubation chamber containing aCSF (in mM: 126 NaCl, 2.5 KCl, 1.25 NaH<sub>2</sub>PO<sub>4</sub>, 2 MgCl<sub>2</sub>, 2 CaCl<sub>2</sub>, 26 NaHCO<sub>3</sub>, and 10 glucose) held at 34°C for 30 min before moving to aCSF at room temperature until used for recordings. Recordings were made from a submersion chamber perfused with aCSF (2 ml/min) held at 32°C.

### Electrophysiology

Borosilicate glass electrodes (3–6 M $\Omega$ ) were filled with K-gluconate internal solution (in mM: 115 potassium gluconate, 20 KCl, 1.5 MgCl<sub>2</sub>, 10 phosphocreatine-Tris, 2 MgATP, and 0.5 Na<sub>3</sub>GTP; pH 7.2–7.4, 280–285 mOsm). GFP-positive cells in the dorsal CA1 region of HPC were visualized using an upright microscope (Olympus) using infrared and epifluorescent illumination. CA1 pyramidal cells were distinguished by location in the cell body layer and individual cell morphology. Whole-cell patch-clamp recordings were made from transfected cells using a Multiclamp 700B amplifier and a Digidata 1440A digitizer (Molecular Devices), and whole-cell junction potential was not corrected. Traces were sampled (10 kHz), filtered (10 kHz), and digitally stored. Cells with membrane potential more positive than –50 mV or series resistance of >20 M $\Omega$  were omitted from analysis. Series resistance was

measured as the sum of the access resistance ( $M\Omega$ ) and the tip resistance ( $M\Omega$ ).

Membrane capacitance, membrane resistance, and access resistance were measured according to the pClamp 10 manual (Molecular Devices). Briefly, the membrane capacitance, membrane resistance, and access resistance were determined by fitting the transient portion of the current response in the pClamp membrane test to an exponential function. Integrating this function yielded the area under the curve of the current response, and its components were automatically analyzed to determine the above membrane parameters. Input resistance was measured in Clampfit (Molecular Devices) from a current clamp input–output curve as the slope of the line fitted to the voltages recorded at increasing current injections (first voltage,  $<120$  mV). Resting membrane potential (in mV) was read using the Multiclamp 700B Commander (Molecular Devices) while injecting no current ( $I = 0$ ) immediately after breaking into a cell to avoid the error generated by the voltage drop across the resistance of the recording electrode during current injection. Bridge-balance compensation was not used in the above determination of membrane parameters.

Rheobase was measured by giving brief (250 ms) depolarizing (5 pA) steps with 250 ms between steps. The elicited action potential (AP) number was measured by issuing increasing depolarizing steps (25–300 pA, 500 ms) with 500 ms in between steps. For measures of hyperpolarization-activated cation current ( $I_h$ ), hyperpolarizing steps (500 ms) that produced potentials at  $-130$  to  $-50$  mV were issued in between the holding current. For synaptic recordings of spontaneous EPSCs (sEPSCs), cells were held at  $-80$  mV for 2 min. Evoked EPSCs were conducted at  $-70$  and  $+40$  mV using a digital stimulator (Digitimer) and a tungsten stimulating electrode (50–500  $\mu$ A, 50  $\mu$ s; World Precision Instruments) placed locally in the stratum radiatum layer of CA1 to target Schaffer collateral fibers. All electrophysiology recordings were made at  $\sim 30$ – $32^\circ\text{C}$  by warming the aCSF line with a single inline heater (Warner Instruments).

### Data analysis

All traces were analyzed using pClamp (Clampfit; RRID: SCR\_011323). Compiled data were analyzed using mixed two-way repeated-measures ANOVAs or one-way ANOVAs followed by Holm–Sidak-corrected multiple comparisons. Rheobase was taken as the lowest step necessary to elicit a spike. Spike frequency adaptation was measured from elicited action potentials at the maximal current step as the interspike interval (ISI; in ms). For measures of  $I_h$ , peak and steady-state (S.S.) potential were obtained from the antipeak and for the last 20 ms of the step, respectively.  $I_h$  was measured at the maximal negative current necessary to hyperpolarize the cell to  $-120$  mV. For sEPSCs, measurements across a 2 min trace were analyzed by Mini Analysis (Synaptosoft) and filtered with a low-pass Butterworth filter (500 Hz). sEPSCs with peak amplitudes not readily distinguishable from noise ( $\leq 5$  pA) were excluded from the analysis. For AMPA/NMDA ratio, data for each cell were averaged from

10 evoked EPSCs. For EPSCs at  $-70$  mV, peak amplitude was measured. For EPSCs at  $+40$  mV, amplitude was measured 40 ms after stimulation to isolate NMDA current from the more transient AMPA current. Cells with low peak amplitude AMPA EPSCs ( $<100$  pA at highest stimulus intensity) and/or low amplitude NMDA EPSCs ( $<100$  pA at 50 ms after highest stimulus intensity) were excluded from the analysis. NMDA decay tau was determined based on previously established methods (Cathala et al., 2000). We averaged NMDA EPSCs (10–15 traces) and fitted the decay portion based on the following equation:

$$A(t) = A_{\text{slow}} * e^{-t/\tau_{\text{slow}}} + A_{\text{fast}} * e^{-t/\tau_{\text{fast}}},$$

where  $\tau_{\text{slow}}$  and  $\tau_{\text{fast}}$  represent the decay time constants and  $A_{\text{slow}} + A_{\text{fast}}$  represent the amplitudes of the slow and fast components. We then calculated the weighted time constant ( $\tau_w$ ) based on the following equation:

$$t_w = t_{\text{slow}} * [A_{\text{slow}} / (A_{\text{slow}} + A_{\text{fast}})] + t_{\text{fast}} * [A_{\text{fast}} / (A_{\text{slow}} + A_{\text{fast}})].$$

## Results

### $\Delta$ FosB decreases intrinsic membrane excitability of CA1 neurons

To determine the role of  $\Delta$ FosB in regulating dHPC CA1 pyramidal cell function, we examined the effects of viral-mediated overexpression and inhibition of  $\Delta$ FosB on intrinsic excitability and measures of synaptic strength (Fig. 1A). We first tested whether HSV-mediated overexpression of GFP and  $\Delta$ FosB, or  $\Delta$ JunD, an inhibitor of  $\Delta$ FosB transcriptional regulation, affected basic cell and membrane properties. No changes were observed in resting membrane potential, membrane resistance, access (series) resistance, membrane capacitance, or input resistance (Table 1).

To measure excitability, CA1 pyramidal cells were injected with increasing steps (500 ms) of current ( $\Delta 25$  pA/step) with periods of rest (0 pA, 500 ms) in between the steps. Representative voltage traces to a 125 pA current step are shown in Figure 1B.  $\Delta$ FosB overexpression decreased the number of spikes observed across steps (Fig. 1C; main effect of group:  $F_{(2,51)} = 10.12$ ,  $p < 0.001$ ; Fig. 1C, inset: GFP vs  $\Delta$ FosB,  $p = 0.024$ , 75–250 pA:  $p < 0.05$  compared with GFP). No differences were observed in spike amplitude or half-width (data not shown), indicating that  $\Delta$ FosB did not modify action potential kinetics.  $\Delta$ FosB also increased the threshold necessary to elicit an AP (rheobase) in response to a brief depolarizing step of current (Fig. 1D;  $F_{(2,51)} = 5.73$ ,  $p = 0.006$ ;  $p = 0.044$  compared with GFP).

Additionally,  $\Delta$ FosB antagonism exerted an opposite effect, increasing excitability.  $\Delta$ JunD, a dominant negative mutant of the binding partner of  $\Delta$ FosB, JunD, which binds to endogenous  $\Delta$ FosB and antagonizes transcriptional activity by preventing transactivation (Peakman et al., 2003), caused a persistent increase in AP number across depolarizing steps (Fig. 1C, inset: GFP vs  $\Delta$ JunD,  $p = 0.035$ ; Fig. 1C: 75–250 pA,  $p < 0.05$  compared with GFP), while having no effect on rheobase (Fig. 1D). These

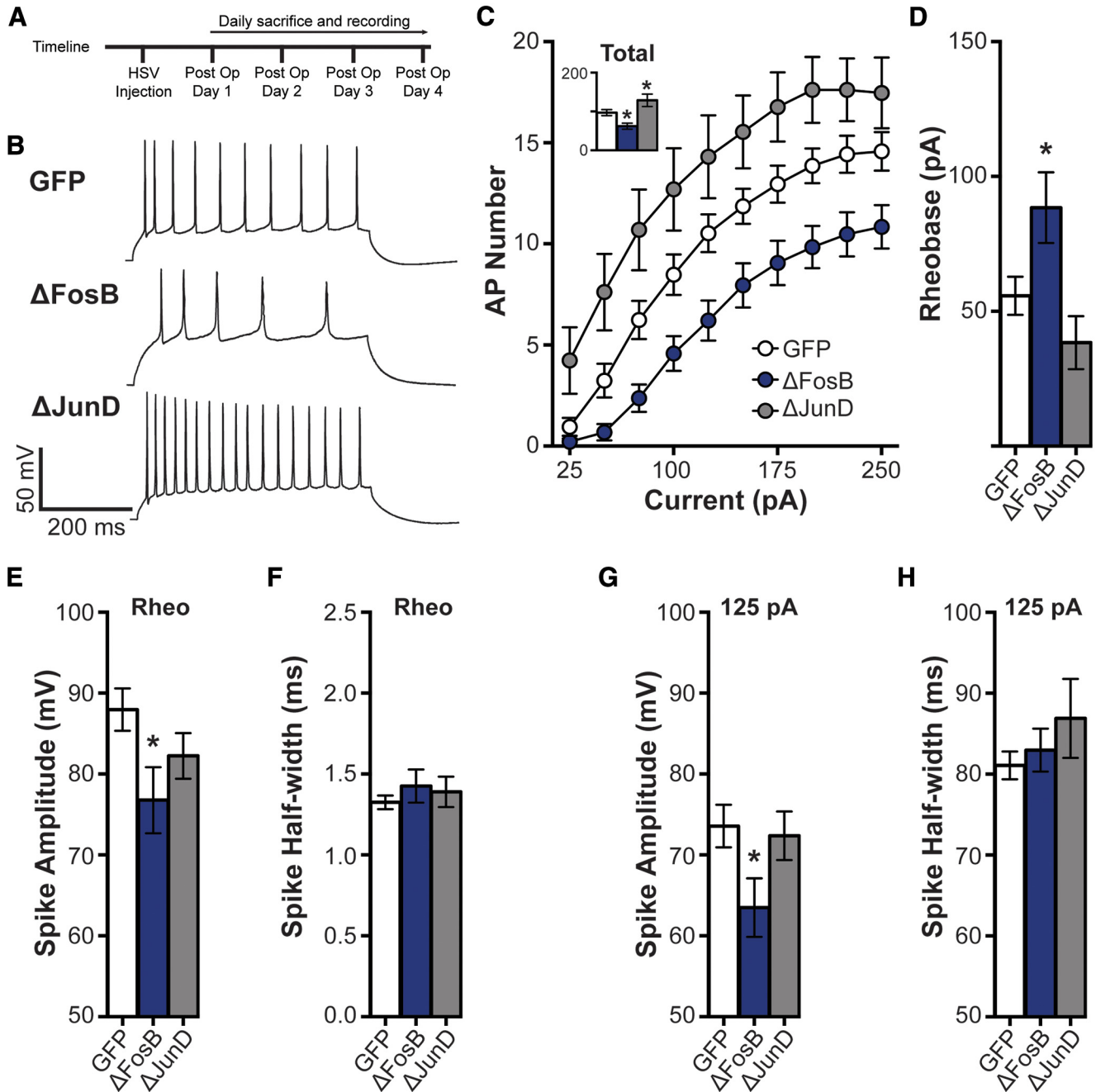


**Figure 1.**  $\Delta$ FosB regulates spike number in hippocampal CA1 neurons. **A**, Experimental timeline. **B**, Representative spikes from 125 pA depolarizing current injection in dHPC CA1 neurons transduced by HSV-GFP (GFP), HSV-GFP+ $\Delta$ FosB ( $\Delta$ FosB), and HSV-GFP +  $\Delta$ JunD ( $\Delta$ JunD). **C**, Spike (AP) number across increasing depolarizing current steps (25–250 pA) for GFP ( $n = 21$  cells;  $n = 8$  mice),  $\Delta$ FosB ( $n = 19$  cells;  $n = 9$  mice), and  $\Delta$ JunD ( $n = 14$  cells;  $n = 5$  mice). The number of APs was significantly decreased by  $\Delta$ FosB, and increased by  $\Delta$ JunD.  $*p < 0.05$ ,  $**p < 0.01$  (two-way repeated-measures ANOVA; Holm–Sidak comparisons). Inset, Total number of APs across all steps. Total spikes were similarly regulated by  $\Delta$ FosB.  $*p < 0.05$  (one-way ANOVA; Holm–Sidak comparisons). **D**, Rheobase (in pA) in GFP-,  $\Delta$ FosB-, and  $\Delta$ JunD-expressing cells. Rheobase was significantly increased by  $\Delta$ FosB expression.  $*p < 0.05$  (one-way ANOVA; Holm–Sidak comparisons). **E**, Rheobase spike peak amplitude (in mV). Spike amplitude was significantly decreased by  $\Delta$ FosB expression.  $*p < 0.05$  (one-way ANOVA; Holm–Sidak comparisons). **F**, Rheobase spike half-width (in ms). No differences were observed. **G**, Mean spike amplitude (in mV) elicited by 125 pA depolarizing current injection. Spike amplitudes at 125 pA current were significantly decreased by  $\Delta$ FosB expression.  $*p < 0.05$  (one-way ANOVA; Holm–Sidak comparisons). **H**, Mean spike half-width (in ms) elicited by 125 pA depolarizing current injection. No differences were observed. All graphs display means  $\pm$  SEM.

**Table 1** Effects of  $\Delta$ FosB overexpression or inhibition on properties of dorsal CA1 neurons.

Cell property	GFP ( <i>n</i> = 21)	$\Delta$ FosB ( <i>n</i> = 19)	$\Delta$ JunD ( <i>n</i> = 14)
Resting potential (mV)	$-66.7 \pm 0.7$	$-67.9 \pm 1.1$	$-66.3 \pm 14.4$
Membrane capacitance (pF)	$71.6 \pm 4.6$	$66.4 \pm 5.4$	$60.0 \pm 5.9$
Membrane resistance (M $\Omega$ )	$66.1 \pm 9.0$	$58.9 \pm 10.4$	$67.9 \pm 7.9$
Access resistance (M $\Omega$ )	$18.7 \pm 1.2$	$19.3 \pm 1.3$	$18.7 \pm 1.9$
Input resistance (M $\Omega$ )	$156.7 \pm 11.9$	$171.9 \pm 25.6$	$176.6 \pm 15.2$

Values are reported as the mean  $\pm$  SEM.

findings suggest that endogenous  $\Delta$ FosB decreases the intrinsic membrane excitability of dHPC CA1 neurons.

### Spike amplitude is decreased by $\Delta$ FosB expression

We next assessed the properties of the action potential: peak amplitude (in mV) and duration (half-width, in ms). We examined spike properties at both rheobase and the average spike properties of all spikes elicited by a 125 pA current injection (as shown in the representative traces in Fig. 1B). Spike amplitude at rheobase was significantly decreased by  $\Delta$ FosB expression (Fig. 1E; one-way ANOVA:  $F_{(2,50)} = 3.26$ ,  $p = 0.047$ ; *post hoc*:  $p = 0.028$ ), and this was also observed at the 125 pA current step (Fig. 1G; one-way ANOVA:  $F_{(2,49)} = 3.25$ ,  $p = 0.047$ ; *post hoc*:  $p = 0.039$ ).  $\Delta$ JunD expression did not significantly alter spike amplitude. In addition, no differences were observed in spike duration at rheobase (Fig. 1F) or 125 pA current (Fig. 1G). Thus,  $\Delta$ FosB overexpression in CA1 neurons appears to decrease the peak amplitude of action potentials.

### Spike frequency adaptation is enhanced by $\Delta$ FosB expression

Excitability may reflect changes in spike frequency adaptation as a result of differential ion channel expression (Storm, 1990; Fleidervish et al., 1996; Gu et al., 2007). Thus,  $\Delta$ FosB may mediate intrinsic mechanisms (e.g., ion channel expression and/or function), which influence cellular excitability in CA1 neurons by increasing spike adaptation across depolarizing current or by changes in hyperpolarization-activated current. Therefore, we investigated spike adaptation (measured by ISI) in elicited APs at the maximal depolarizing current step in GFP-, GFP +  $\Delta$ FosB-, and GFP +  $\Delta$ JunD-expressing CA1 neurons. Groups did not differ in their maximal depolarizing step current (Fig. 2A). At this step,  $\Delta$ FosB overexpression increased mean ISI (Fig. 2B; one-way ANOVA:  $F_{(2,48)} = 5.73$ ,  $p = 0.006$ ; *post hoc*:  $p = 0.039$ ), decreased AP number (Fig. 2C; one-way ANOVA:  $F_{(2,50)} = 4.60$ ,  $p = 0.015$ ; *post hoc*:  $p = 0.048$ ), and increased the latency from the onset of the step and the first spike (Fig. 2D; one-way ANOVA:  $F_{(2,48)} = 4.06$ ,  $p = 0.023$ ; *post hoc*:  $p = 0.047$ ). Therefore, the maximal step was determined to be the ideal current to investigate whether the overall decrease in spike frequency by  $\Delta$ FosB overexpression was due to altered spike adaptation.

We next assessed the ISI for the first and last spike pairs at the maximal step (Fig. 2E). All groups increased ISI at the last spike pair compared with the first spike pair (main effect of spike pair:  $F_{(1,48)} = 75.43$ ,  $p < 0.001$ ). No

differences were found between groups at the first pair of spikes; however,  $\Delta$ FosB significantly increased ISI at the last pair of spikes (interaction of spike pair  $\times$  group:  $F_{(2,48)} = 4.95$ ,  $p = 0.011$ ; *post hoc*:  $p = 0.003$  compared with GFP). This suggests that the  $\Delta$ FosB reduction of CA1 neuron excitability may be due to an enhancement in spike frequency adaptation.

### $\Delta$ FosB overexpression decreases hyperpolarization-activated current in CA1 neurons

Hippocampal neuron activity, like that produced by theta burst stimulation, can produce decreases in cellular, but not dendritic, excitability that are associated with increased  $I_h$  (Fan et al., 2005). Therefore, we also examined the effects of  $\Delta$ FosB on  $I_h$  in dHPC CA1 neurons. Representative hyperpolarizing voltage traces displaying peak voltage and S.S. for CA1 cells expressing GFP, GFP +  $\Delta$ FosB, and GFP +  $\Delta$ JunD are shown in Figure 3A–C. Across hyperpolarizing steps, GFP cells show voltage differences between peak and S.S. (Fig. 3D; interaction of state  $\times$  step:  $F_{(5,204)} = 8.98$ ,  $p < 0.001$ ;  $p < 0.001$  between peak and S.S. across  $-500$  to  $-200$  pA hyperpolarizing steps), indicative of  $I_h$  that is normally observed in CA1 pyramidal neurons (Maccaferri et al., 1993; Magee, 1999). However,  $\Delta$ FosB decreased these differences across current steps (Fig. 3E;  $p > 0.05$  for interaction of state  $\times$  step;  $p < 0.05$  between peak and S.S. at only  $-400$  and  $-300$  hyperpolarizing steps). The antagonism of  $\Delta$ FosB by  $\Delta$ JunD may have also mildly reduced  $I_h$  compared with GFP, indicated by lower mean differences between peak and S.S. across hyperpolarizing steps (Fig. 3F, bottom;  $p > 0.05$  for interaction of state  $\times$  step;  $p < 0.05$  between peak and S.S. across  $-400$  to  $-200$  pA hyperpolarizing steps).

We also examined  $I_h$  at the maximal negative current step (see Materials and Methods), which did not differ between groups (Fig. 3G,H;  $p > 0.05$ ). At this step,  $\Delta$ FosB significantly reduced the difference between peak and S.S. (Fig. 3I; one-way ANOVA:  $F_{(2,49)} = 4.83$ ,  $p = 0.012$ ; *post hoc*:  $p = 0.006$  compared with GFP) and the sag ratio (calculated as S.S./peak; Fig. 3J; one-way ANOVA:  $F_{(2,49)} = 4.17$ ,  $p = 0.021$ ; *post hoc*:  $p = 0.012$  compared with GFP). These findings suggest that  $I_h$  is regulated by  $\Delta$ FosB, which may contribute to the change in excitability; however, the blockade of  $\Delta$ FosB does not appear to sufficiently alter basal  $I_h$  values in CA1 neurons to account for the increased excitability observed in Figure 1. This, along with the finding that  $\Delta$ JunD does not regulate spike adaptation, suggests that enhanced excitability caused

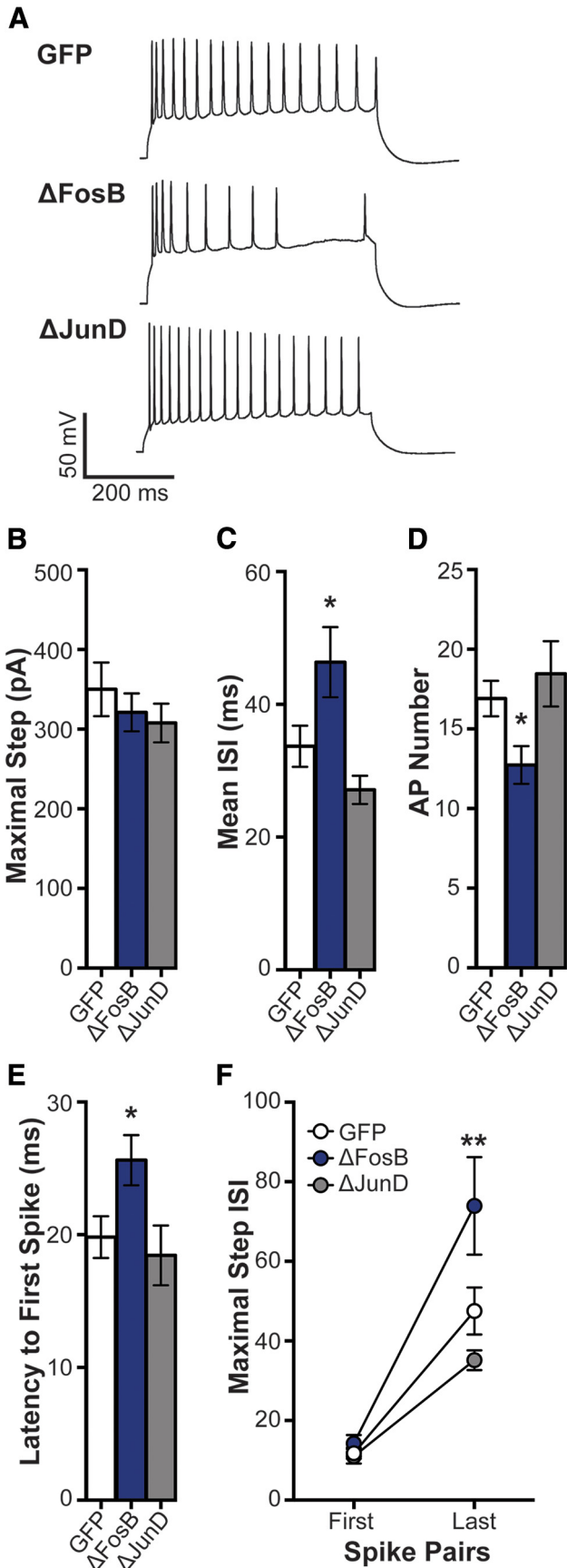


**Figure 2.** ΔFosB enhances spike frequency adaptation. **A**, Rep-

Figure 2. continued

representative spikes at maximal depolarizing current injection in dHPC CA1 neurons transduced by HSV-GFP (GFP), HSV-GFP + ΔFosB (ΔFosB), and HSV-GFP + ΔJunD (ΔJunD). **B**, The maximal depolarizing current was used to assess spike frequency adaptation among GFP ( $n = 21$  cells;  $n = 8$  mice), ΔFosB ( $n = 19$  cells;  $n = 9$  mice), and ΔJunD ( $n = 14$  cells;  $n = 5$  mice). No differences were observed in maximal current;  $p > 0.05$  (one-way ANOVA). **C**, Mean ISI (in ms) at the maximal step across groups. Mean ISI was increased by ΔFosB;  $*p < 0.05$  compared with GFP (one-way ANOVA; Holm–Sidak comparisons). **D**, Number of APs at the maximal step across groups. ΔFosB significantly decreased the number APs;  $*p < 0.05$  compared with GFP (one-way ANOVA; Holm–Sidak comparisons). **E**, Latency from the onset of the maximal step and the first spike was assessed for each group. ΔFosB increased the latency compared with GFP;  $*p < 0.05$  (one-way ANOVA; Holm–Sidak comparisons). **F**, ISI for the first and last pair of spikes at the maximal step for each group. ISI at the last pair of spikes was increased by ΔFosB compared with GFP;  $**p < 0.01$  (two-way repeated-measures ANOVA; Holm–Sidak comparisons). All graphs display means  $\pm$  SEM.

by ΔFosB antagonism may be driven by different mechanisms than spike adaptation or  $I_h$ .

**ΔFosB alters synaptic strength in CA1 neurons**

ΔFosB increases dendritic spine formation in NAc and dHPC, and produces cell type-specific adaptations in synaptic strength in NAc MSNs (Grueter et al., 2013; Eagle et al., 2015). This suggests that ΔFosB may also regulate functional synaptic plasticity in dHPC CA1 neurons. Therefore, we sought to assess the role of ΔFosB in sEPSCs and AMPA/NMDA ratios in CA1 neurons. sEPSCs were assessed at  $-80$  mV over 2 min periods. Representative traces of sEPSCs are shown in Figure 4A. No changes were observed in the sEPSC frequency (Fig. 4B), but both ΔFosB and ΔJunD decreased sEPSC amplitudes (Fig. 4C,D;  $F_{(2,42)} = 4.75$ ,  $p = 0.014$ ;  $p = 0.027$  for ΔFosB and  $p = 0.027$  for ΔJunD compared with GFP, respectively), suggesting that both ΔFosB overexpression and antagonism may reduce the postsynaptic response in CA1 neurons.

To directly assess whether ΔFosB regulates postsynaptic strength in CA1 neurons, we examined glutamate receptor function using AMPA/NMDA ratios of evoked EPSCs. Representative traces of evoked EPSCs at  $-70$  and  $+40$  mV are shown in Figure 5A. Interestingly, ΔJunD-mediated antagonism of ΔFosB significantly increased the AMPA/NMDA ratio (Fig. 5B;  $F_{(2,39)} = 4.41$ ,  $p = 0.023$ ;  $p = 0.038$  compared with GFP), but no differences were found by ΔFosB overexpression. This ΔJunD-driven increase in AMPA/NMDA ratio, which is usually interpreted as an increase in synaptic strength, is in stark contrast to the ΔJunD-driven decrease in sEPSC amplitude (Fig. 4). Therefore, we also assessed the kinetic

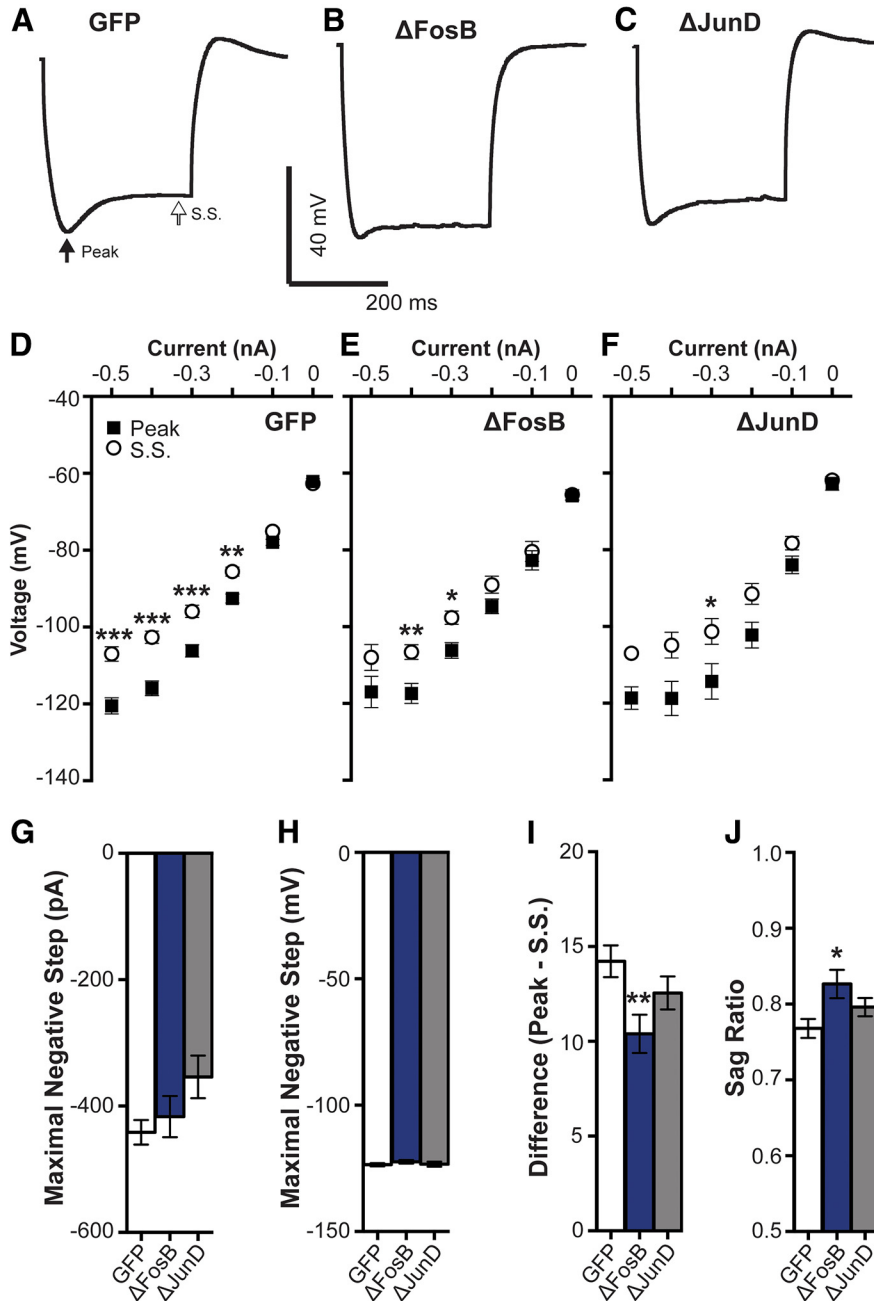


**Figure 3.**  $\Delta$ FosB decreases  $I_h$ . **A–C**, Representative voltage trace to a hyperpolarizing current step showing  $I_h$  in hippocampal CA1 neurons expressing GFP ( $n = 21$  cells;  $n = 8$  mice),  $\Delta$ FosB ( $n = 19$  cells;  $n = 9$  mice), and  $\Delta$ JunD ( $n = 13$  cells;  $n = 5$  mice), respectively. Arrows indicate amplitude measured at peak and S.S. **D–F**,  $I$ - $V$  curves from hyperpolarizing current injections (0 to  $-500$  pA) at peak and S.S. in GFP,  $\Delta$ FosB, and  $\Delta$ JunD cells. GFP cells had significant differences between peak and S.S. across currents (from  $-500$  to  $-200$  pA), indicative of  $I_h$ ,  $***p < 0.001$  (two-way ANOVA; Holm–Sidak comparisons). Differences between peak and S.S. were comparably reduced in both  $\Delta$ FosB (only different at steps  $-400$  and  $-300$  pA) and  $\Delta$ JunD groups (only at  $-300$  pA), indicative of reduced  $I_h$ ,  $*p < 0.05$ ,  $**p < 0.01$  (two-way ANOVAs; Holm–Sidak comparisons). **G**, **H**, Mean maximal negative current and voltage (produced by maximal negative current), respectively, in GFP,  $\Delta$ FosB, and  $\Delta$ JunD cells. No differences were observed between groups;  $p > 0.05$  (one-way ANOVA). **I**, Difference between peak and S.S. at maximal negative current across groups.  $\Delta$ FosB significantly decreased the difference compared with GFP;  $**p < 0.01$  (one-way ANOVA; Holm–Sidak comparisons). **J**, Sag ratio (S.S./peak at maximal negative current ratio) across groups.  $\Delta$ FosB significantly increased the sag ratio (decreased  $I_h$ ) compared with GFP;  $*p < 0.05$  (one-way ANOVA; Holm–Sidak comparisons). All graphs display means  $\pm$  SEM.

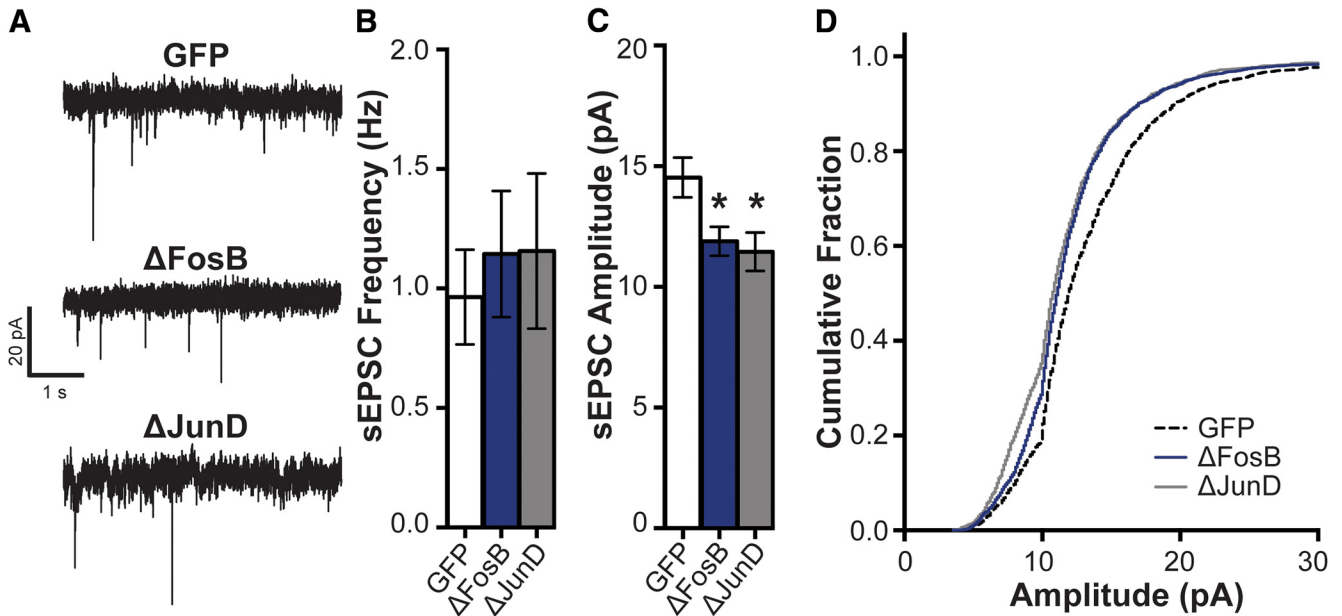


**Figure 4.** ΔFosB decreases spontaneous EPSC amplitude. **A**, Representative traces (−80 mV) showing sEPSCs in hippocampal CA1 neurons expressing GFP ( $n = 20$  cells;  $n = 7$  mice), ΔFosB ( $n = 16$  cells;  $n = 6$  mice), and ΔJunD ( $n = 9$  cells;  $n = 5$  mice). **B**, sEPSC frequency (in Hz) across groups. No differences in sEPSC frequency were observed. **C**, sEPSC peak amplitude (in pA) across groups. Both ΔFosB and ΔJunD reduced sEPSC amplitude compared with GFP;  $*p < 0.05$  (one-way ANOVA; Holm–Sidak comparisons). **D**, Cumulative fraction of the peak amplitudes (5–30 pA) across groups. Both ΔFosB and ΔJunD were shifted to the left from GFP. All graphs display means  $\pm$  SEM.

properties of the evoked EPSCs. We did not detect any differences in the AMPA-mediated amplitude of evoked EPSCs at −70 mV; however, the decay time constant of the NMDA-mediated current was significantly reduced by ΔJunD overexpression (Fig. 5C;  $F_{(2,39)} = 6.87$ ,  $p =$

0.003;  $p = 0.011$  compared with GFP). This suggests that antagonism of ΔFosB produces a decreased NMDA current, potentially via changes in receptor subunit composition, leading to the apparent increase in AMPA/NMDA ratios.

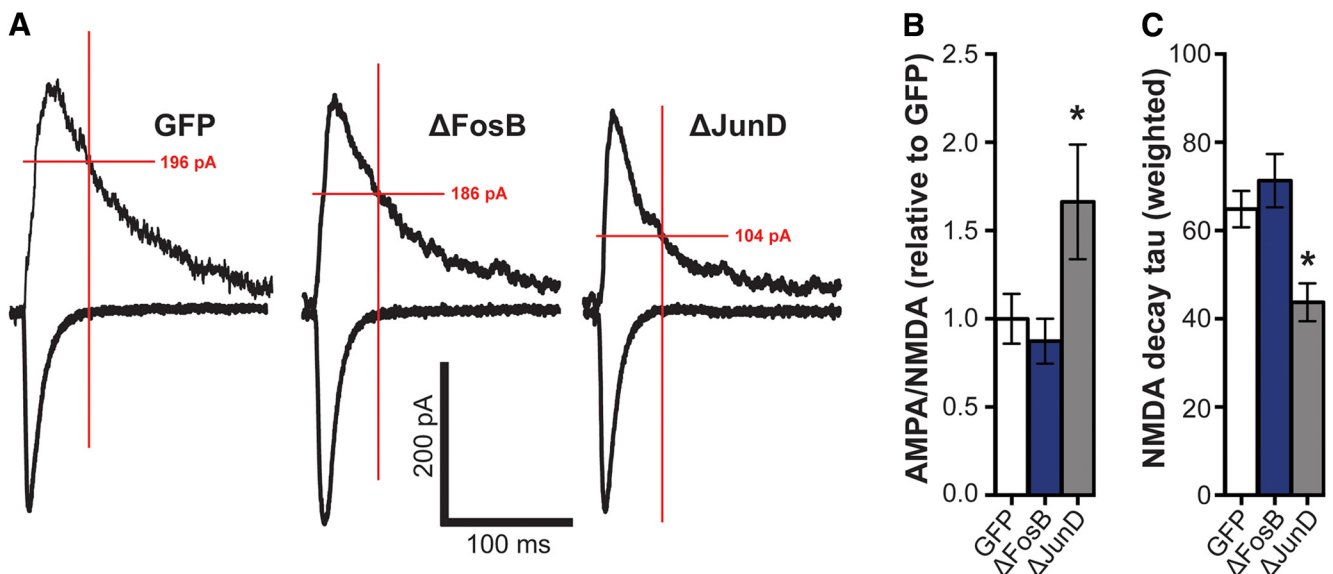


**Figure 5.** Blockade of ΔFosB enhances AMPA/NMDA ratio. **A**, Representative average number of evoked EPSCs at −70 and +40 mV in dHPC CA1 neurons expressing GFP ( $n = 19$  cells;  $n = 8$  mice), ΔFosB ( $n = 13$  cells;  $n = 9$  mice), and ΔJunD ( $n = 10$  cells;  $n = 4$  mice). Red lines indicate the measurement for NMDA currents, 50 ms after stimulation. **B**, AMPA/NMDA ratios (normalized relative to GFP) across groups. ΔJunD significantly increased the AMPA/NMDA ratio compared with GFP. **C**, Decay tau for NMDA currents (weighted across both fast and slow components) across groups. ΔJunD significantly reduced NMDA decay tau;  $*p < 0.05$  (one-way ANOVA; Holm–Sidak comparisons). All graphs display means  $\pm$  SEM.



## Discussion

We demonstrate that  $\Delta$ FosB overexpression decreases the excitability of dHPC CA1 pyramidal neurons, and, conversely, antagonism of endogenous  $\Delta$ FosB function increases excitability. This is the first study to suggest that an activity-dependent transcription factor decreases excitability in these cells and raises the question of whether this is mediated by direct transcriptional regulation of ion channel expression or via regulation of other intermediary signaling or transcriptional regulators, such as the  $\Delta$ FosB targets CaMKII or c-Fos (Robison et al., 2013, 2014; You et al., 2017).  $\Delta$ FosB could be directly downregulating the expression of specific Na<sup>+</sup> channels, or could achieve their downregulation indirectly by repression of immediate early genes, such as c-fos, which regulate Na<sup>+</sup> channel expression. For example,  $\Delta$ FosB represses c-fos expression via histone deacetylation (Renthal et al., 2008; You et al., 2017), which has been observed recently in dentate gyrus hippocampal neurons (Corbett et al., 2017). Alternatively,  $\Delta$ FosB may be enhancing the expression or function of ion channels associated with decreased excitability (e.g., K<sup>+</sup> channels). However, target genes of  $\Delta$ FosB in hippocampus have not yet been fully delineated.

Homeostatic changes in excitability are associated with enhanced synaptic strengthening, typically after repeated neuronal activity or learning (Desai et al., 1999; Zhang and Linden, 2003), and this is regulated by both transcriptional and epigenetic mechanisms (Schulz et al., 2008; Guzman-Karlsson et al., 2014; Meadows et al., 2015, 2016). Thus, the reduction in excitability may be a compensatory cellular mechanism resulting from enhanced dendritic or synaptic activity, although future studies are needed to fully determine the role of  $\Delta$ FosB in synaptic plasticity. However, this idea raises interesting possibilities that the  $\Delta$ FosB-driven reduction in excitability may contribute to homeostatic mechanisms producing decreased global activity, thereby enabling the fine tuning of synapses after experience. Furthermore, the role of hippocampal  $\Delta$ FosB in learning (Eagle et al., 2015; Corbett et al., 2017) indicates that this may be linked to experience-driven changes underlying memory consolidation. Excitability was recently hypothesized to be linked to place cell selectivity and memory allocation (Schmidt-Hieber and Nolan, 2017). In this hypothesis, increased excitability distinguishes place cells amid pools of “silent” non-place cells. Therefore,  $\Delta$ FosB induction and its subsequent effects on excitability may act as a mechanism enhancing signal-to-noise in the pool of place-to-silent cells. Additionally, potential fine tuning of hippocampal plasticity of  $\Delta$ FosB, both intrinsic and synaptic, may be aberrant in neurologic diseases, such as Alzheimer’s disease and epilepsy, and contribute to cognitive dysfunction (Corbett et al., 2017; You et al., 2017).

We also demonstrated that the decrease in excitability was associated with a concurrent decrease in  $I_h$  and an increase in spike frequency adaptation.  $I_h$  regulates excitability (van Welie et al., 2004; Fan et al., 2005; Kim Chung et al., 2012), primarily by homeostatically decreasing excitability after synaptic strengthening from neuronal activity (van Welie et al., 2004; Brager and Johnston, 2007).

Therefore, these findings indicate that  $I_h$  may be contributing to the  $\Delta$ FosB-mediated change in excitability. However, because  $I_h$  is typically associated with an increase in excitability (Fan et al., 2005; Kim Chung et al., 2012), the decreased  $I_h$  we observe may not be causally related to the change in excitability and may reflect  $\Delta$ FosB-mediated transcription of targets that separately reduce both excitability and  $I_h$ . Future studies using pharmacological isolation and blockade of  $I_h$  will be needed to determine the relationship between the effects of  $\Delta$ FosB on  $I_h$  and excitability.

It is also possible that the reduction in excitability is driven by a  $\Delta$ FosB-mediated increase in spike frequency adaptation. Spike adaptation is typically regulated by M-type K<sup>+</sup> currents or inactivation of depolarizing currents (Storm, 1990; Benda and Herz, 2003; Otto et al., 2006; Gu et al., 2007). Additionally, the concurrent change in excitability and spike frequency adaptation may be driven by changes in membrane voltage (Fernandez et al., 2011), but this is unlikely as we did not observe a change in resting membrane potential.  $\Delta$ FosB may therefore be transcriptionally activating or silencing targets that regulate spike adaptation (i.e., Na<sup>+</sup> or K<sup>+</sup> channels), which may, in part, underlie the decrease in excitability. During a depolarization, Na<sup>+</sup> channels are inactivated and recover only gradually, contributing to spike adaptation and a decrease in spike amplitude (Benda and Herz, 2003).  $\Delta$ FosB could be acting to either prematurely inactivate Na<sup>+</sup> channels or depress the recovery of Na<sup>+</sup> channels. This potential mechanism would support a decrease in spike adaptation as well as the decrease in spike amplitude. These findings collectively point to  $\Delta$ FosB regulating intrinsic membrane excitability in CA1 neurons, and future studies will uncover the specific transcriptional targets and downstream mechanisms driving this phenomenon.

The finding that  $\Delta$ JunD antagonism of  $\Delta$ FosB increased AMPA/NMDA ratios while decreasing sEPSC amplitude appears contradictory at first pass; however, this change in AMPA/NMDA ratio is likely explained by a decreased NMDA-mediated current rather than an increased AMPA current. NMDAR decay kinetics are determined in part by receptor subunit composition, with GluN2A-containing receptors having much faster decay than GluN2B- or GluN2C-containing receptors (Vicini et al., 1998). It is interesting to speculate that  $\Delta$ FosB may be regulating the expression of the *GRIN2A* or *GRIN2B* genes in hippocampal CA1 neurons, a function that  $\Delta$ FosB does not appear to have in NAc MSNs (Kelz et al., 1999; Robison et al., 2013). Future experiments examining  $\Delta$ FosB gene targets in hippocampal pyramidal neurons, potentially including chromatin immunoprecipitation and gene expression studies, will be required to determine whether NMDAR subunit expression is indeed directly regulated by  $\Delta$ FosB.

Together, the decreased sEPSC amplitude and NMDA-mediated current makes it likely that antagonism of  $\Delta$ FosB leads to decreased synaptic strength.  $\Delta$ JunD has been previously identified to decrease the total number as well as the number of mature, mushroom-shaped dendritic spines in dorsal CA1 neurons (Eagle et al., 2015), a structural phenomenon associated with reduced synaptic

strength (Ziv and Smith, 1996; Engert and Bonhoeffer, 1999; Toni et al., 2007). Changes in synaptic strength in dorsal CA1, such as decreased NMDAR function and/or expression, are associated with a variety of impairments in learning and memory (McHugh et al., 1996; Tsien et al., 1996; Wilson and Tonegawa, 1997). Supporting this,  $\Delta$ FosB antagonism by  $\Delta$ JunD is known to impair spatial and contextual learning (Eagle et al., 2015). Thus, the current findings suggest that  $\Delta$ FosB transcriptional activity is necessary for dorsal CA1-mediated synaptic plasticity underlying memory consolidation, potentially via direct action on NMDAR gene expression.

In addition to learning and memory,  $\Delta$ FosB is also robustly induced in hippocampus by antidepressants, such as fluoxetine (Vialou et al., 2015), suggesting that it may underlie resilience to stress and depressive phenotypes. These novel findings suggest that a potential mechanism for antidepressant effects may be a decrease in the excitability of hippocampal neurons. Antidepressants, particularly selective serotonin reuptake inhibitors, have anticonvulsant properties (Yan et al., 1994; Favale et al., 1995; Wada et al., 1995), which may be mediated by decreased excitability through the inhibition of various  $\text{Ca}^{2+}$  and/or  $\text{K}^{+}$  channels (Deák et al., 2000; Choi et al., 2004; Igelström and Heyward, 2012) either indirectly or via serotonergic mechanisms (Andrade, 2011). Similarly,  $\Delta$ FosB is also induced in HPC by chronic exposure to drugs of abuse (Perrotti et al., 2008), and it has been found that chronic amphetamine use reduces the intrinsic excitability of ventral subiculum neurons (Cooper et al., 2003). Therefore,  $\Delta$ FosB may act as a critical regulator of general hippocampal excitability under a variety of disease conditions, from depression to addiction, or in specific ensembles of CA1 neurons during learning. Future studies will determine the gene targets and downstream mechanisms of these effects and delineate their possible roles in both normal and aberrant hippocampal function.

## References

- Alberini CM, Kandel ER (2014) The regulation of transcription in memory consolidation. *Cold Spring Harb Perspect Biol* 7:a021741. [CrossRef](#) [Medline](#)
- Andrade R (2011) Serotonergic regulation of neuronal excitability in the prefrontal cortex. *Neuropharmacology* 61:382–386. [CrossRef](#) [Medline](#)
- Benda J, Herz AVM (2003) A universal model for spike-frequency adaptation. *Neural Comput* 15:2523–2564. [CrossRef](#) [Medline](#)
- Brager DH, Johnston D (2007) Plasticity of intrinsic excitability during long-term depression is mediated through mGluR-dependent changes in  $I_h$  in hippocampal CA1 pyramidal neurons. *J Neurosci* 27:13926–13937. [CrossRef](#)
- Carle TL, Ohnishi YN, Ohnishi YH, Alibhai IN, Wilkinson MB, Kumar A, Nestler EJ (2007) Proteasome-dependent and -independent mechanisms for FosB destabilization: identification of FosB degradation domains and implications for DeltaFosB stability. *Eur J Neurosci* 25:3009–3019. [CrossRef](#) [Medline](#)
- Cates HM, Thibault M, Pfau M, Heller E, Eagle A, Gajewski P, Bagot R, Colangelo C, Abbott T, Rudenko G, Neve R, Nestler EJ, Robison AJ (2014) Threonine 149 phosphorylation enhances  $\Delta$ FosB transcriptional activity to control psychomotor responses to cocaine. *J Neurosci* 34:11461–11469. [CrossRef](#) [Medline](#)
- Cathala L, Misra C, Cull-Candy S (2000) Developmental profile of the changing properties of NMDA receptors at cerebellar mossy fiber-granule cell synapses. *J Neurosci* 20:5899–5905. [Medline](#)
- Choi J-S, Choi BH, Ahn HS, Kim M-J, Han TH, Rhie D-J, Yoon S-H, Jo Y-H, Kim M-S, Hahn SJ (2004) Fluoxetine inhibits A-type potassium currents in primary cultured rat hippocampal neurons. *Brain Res* 1018:201–207. [CrossRef](#) [Medline](#)
- Cooper DC, Moore SJ, Staff NP, Spruston N (2003) Psychostimulant-induced plasticity of intrinsic neuronal excitability in ventral subiculum. *J Neurosci* 23:9937–9946. [Medline](#)
- Corbett BF, You JC, Zhang X, Pyfer MS, Tosi U, Iacono DM, Petrof I, Hazra A, Fu C-H, Stephens GS, Ashok AA, Aschmies S, Zhao L, Nestler EJ, Chin J (2017)  $\Delta$ FosB regulates gene expression and cognitive dysfunction in a mouse model of Alzheimer's disease. *Cell Rep* 20:344–355. [CrossRef](#) [Medline](#)
- Deák F, Lasztóczy B, Pacher P, Petheő GL, Valéria K, Spät A (2000) Inhibition of voltage-gated calcium channels by fluoxetine in rat hippocampal pyramidal cells. *Neuropharmacology* 39:1029–1036.
- Desai NS, Rutherford LC, Turrigiano GG (1999) Plasticity in the intrinsic excitability of cortical pyramidal neurons. *Nat Neurosci* 2:515. [CrossRef](#) [Medline](#)
- Eagle AL, Gajewski PA, Yang M, Kechner ME, Al Masraf BS, Kennedy PJ, Wang H, Mazei-Robison MS, Robison AJ (2015) Experience-dependent induction of hippocampal  $\Delta$ FosB controls learning. *J Neurosci* 35:13773–13783. [CrossRef](#) [Medline](#)
- Eagle AL, Gajewski PA, Robison AJ (2016) Role of hippocampal activity-induced transcription in memory consolidation. *Rev Neurosci* 27:559–573.
- Engert F, Bonhoeffer T (1999) Dendritic spine changes associated with hippocampal long-term synaptic plasticity. *Nature* 399:66. [CrossRef](#) [Medline](#)
- Fan Y, Fricker D, Brager DH, Chen X, Lu H-C, Chitwood RA, Johnston D (2005) Activity-dependent decrease of excitability in rat hippocampal neurons through increases in  $I_h$ . *Nat Neurosci* 8:1542–1551. [CrossRef](#)
- Favale E, Rubino V, Mainardi P, Lunardi G, Albano C (1995) Anticonvulsant effect of fluoxetine in humans. *Neurology* 45:1926–1927. [Medline](#)
- Fernandez FR, Broicher T, Truong A, White JA (2011) Membrane voltage fluctuations reduce spike frequency adaptation and preserve output gain in CA1 pyramidal neurons in a high-conductance state. *J Neurosci* 31:3880–3893. [CrossRef](#)
- Fleiderich IA, Friedman A, Gutnick MJ (1996) Slow inactivation of  $\text{Na}^{+}$  current and slow cumulative spike adaptation in mouse and guinea-pig neocortical neurones in slices. *J Physiol* 493:83–97. [CrossRef](#)
- Frey U, Frey S, Schollmeier F, Krug M (1996) Influence of actinomycin D, a RNA synthesis inhibitor, on long-term potentiation in rat hippocampal neurons in vivo and in vitro. *J Physiol* 490:703–711. [CrossRef](#)
- Grueter BA, Robison AJ, Neve RL, Nestler EJ, Malenka RC (2013) FosB differentially modulates nucleus accumbens direct and indirect pathway function. *Proc Natl Acad Sci U S A* 110:1923–1928. [CrossRef](#) [Medline](#)
- Gu N, Vervaeke K, Storm JF (2007) BK potassium channels facilitate high-frequency firing and cause early spike frequency adaptation in rat CA1 hippocampal pyramidal cells. *J Physiol* 580:859–882. [CrossRef](#) [Medline](#)
- Guzman-Karlsson MC, Meadows JP, Gavin CF, Hablitz JJ, Sweatt JD (2014) Transcriptional and epigenetic regulation of Hebbian and non-Hebbian plasticity. *Neuropharmacology* 80:3–17. [CrossRef](#) [Medline](#)
- Igelström KM, Heyward PM (2012) Inhibition of hippocampal excitability by citalopram. *Epilepsia* 53:2034–2042. [CrossRef](#) [Medline](#)
- Institute of Laboratory Animal Resources (U.S.) (2011) Guide for the care and use of laboratory animals, Ed 8. Washington DC: National Academy of Sciences.
- Kelz MB, Chen J, Carlezon WA Jr, Whisler K, Gilden L, Beckmann AM, Steffen C, Zhang YJ, Marotti L, Self DW, Tkatch T, Baranauskas G, Surmeier DJ, Neve RL, Duman RS, Picciotto MR, Nestler EJ

- (1999) Expression of the transcription factor  $\Delta$ FosB in the brain controls sensitivity to cocaine. *Nature* 401:272–276. [CrossRef](#)
- Kim Chung S, Chang Payne Y, Johnston D (2012) Enhancement of dorsal hippocampal activity by knockdown of HCN1 channels leads to anxiolytic- and antidepressant-like behaviors. *Neuron* 75:503–516. [CrossRef](#)
- Lee JLC, Everitt BJ, Thomas KL (2004) Independent cellular processes for hippocampal memory consolidation and reconsolidation. *Science* 304:839–843. [CrossRef](#)
- Maccaferri G, Mangoni M, Lazzari A, DiFrancesco D (1993) Properties of the hyperpolarization-activated current in rat hippocampal CA1 pyramidal cells. *J Neurophysiol* 69:2129–2136. [CrossRef](#) [Medline](#)
- Magee JC (1999) Dendritic Ih normalizes temporal summation in hippocampal CA1 neurons. *Nat Neurosci* 2:508–514. [CrossRef](#)
- McHugh TJ, Blum KI, Tsien JZ, Tonegawa S, Wilson MA (1996) Impaired hippocampal representation of space in CA1-specific NMDAR1 knockout mice. *Cell* 87:1339–1349. [Medline](#)
- Meadows JP, Guzman-Karlsson MC, Phillips S, Holleman C, Posey JL, Day JJ, Hablitz JJ, Sweatt JD (2015) DNA methylation regulates neuronal glutamatergic synaptic scaling. *Sci Signal* 8:ra61. [CrossRef](#) [Medline](#)
- Meadows JP, Guzman-Karlsson MC, Phillips S, Brown JA, Strange SK, Sweatt JD, Hablitz JJ (2016) Dynamic DNA methylation regulates neuronal intrinsic membrane excitability. *Sci Signal* 9:ra83. [CrossRef](#) [Medline](#)
- Otto JF, Yang Y, Frankel WN, White HS, Wilcox KS (2006) A spontaneous mutation involving Kcnq2 (Kv7.2) reduces M-current density and spike frequency adaptation in mouse CA1 neurons. *J Neurosci* 26:2053–2059. [CrossRef](#) [Medline](#)
- Peakman MC, Colby C, Perrotti LI, Tekumalla P, Carle T, Ulery P, Chao J, Duman C, Steffen C, Monteggia L, Allen MR, Stock JL, Duman RS, McNeish JD, Barrot M, Self DW, Nestler EJ, Schaeffer E (2003) Inducible, brain region-specific expression of a dominant negative mutant of c-Jun in transgenic mice decreases sensitivity to cocaine. *Brain Res* 970:73–86. [Medline](#)
- Perrotti LI, Weaver RR, Robison B, Renthall W, Maze I, Yazdani S, Elmore RG, Knapp DJ, Selley DE, Martin BR, Sim-Selley L, Bachtell RK, Self DW, Nestler EJ (2008) Distinct patterns of  $\Delta$ FosB induction in brain by drugs of abuse. *Synapse* 62:358–369. [CrossRef](#) [Medline](#)
- Renthall W, Carle TL, Maze I, Covington HE, Truong H-T, Alibhai I, Kumar A, Montgomery RL, Olson EN, Nestler EJ (2008)  $\Delta$ FosB mediates epigenetic desensitization of the *c-fos* gene after chronic amphetamine exposure. *J Neurosci* 28:7344–7349. [CrossRef](#) [Medline](#)
- Robison AJ, Vialou V, Mazei-Robison M, Feng J, Kourrich S, Collins M, Wee S, Koob G, Turecki G, Neve R, Thomas M, Nestler EJ (2013) Behavioral and structural responses to chronic cocaine require a feedforward loop involving  $\Delta$ FosB and calcium/calmodulin-dependent protein kinase II in the nucleus accumbens shell. *J Neurosci* 33:4295–4307. [CrossRef](#)
- Robison AJ, Vialou V, Sun HS, Labonte B, Golden SA, Dias C, Turecki G, Tamminga C, Russo S, Mazei-Robison M, Nestler EJ (2014) Fluoxetine epigenetically alters the CaMKII $\alpha$  promoter in nucleus accumbens to regulate  $\Delta$ FosB binding and antidepressant effects. *Neuropsychopharmacology* 39:1178–1186. [CrossRef](#) [Medline](#)
- Schmidt-Hieber C, Nolan MF (2017) Synaptic integrative mechanisms for spatial cognition. *Nat Neurosci* 20:1483. [CrossRef](#) [Medline](#)
- Schulz DJ, Temporal S, Barry DM, Garcia ML (2008) Mechanisms of voltage-gated ion channel regulation: from gene expression to localization. *Cell Mol Life Sci* 65:2215–2231. [CrossRef](#) [Medline](#)
- Squire LR, Barondes SH (1970) Actinomycin-D: effects on memory at different times after training. *Nature* 225:649. [Medline](#)
- Storm JF (1990) Chapter 12 potassium currents in hippocampal pyramidal cells. In: *Progress in brain research* (Storm-Mathisen J, Zimmer J, Ottersen OP, eds), pp 161–187. Amsterdam: Elsevier.
- Toni N, Teng EM, Bushong EA, Aimone JB, Zhao C, Consiglio A, van Praag H, Martone ME, Ellisman MH, Gage FH (2007) Synapse formation on neurons born in the adult hippocampus. *Nat Neurosci* 10:727–734. [CrossRef](#) [Medline](#)
- Tsien JZ, Huerta PT, Tonegawa S (1996) The essential role of hippocampal CA1 NMDA receptor-dependent synaptic plasticity in spatial memory. *Cell* 87:1327–1338. [Medline](#)
- Ulery-Reynolds PG, Castillo MA, Vialou V, Russo SJ, Nestler EJ (2009) Phosphorylation of  $\Delta$ FosB mediates its stability in vivo. *Neuroscience* 158:369–372. [CrossRef](#) [Medline](#)
- van Welie I, van Hooft JA, Wadman WJ (2004) Homeostatic scaling of neuronal excitability by synaptic modulation of somatic hyperpolarization-activated Ih channels. *Proc Natl Acad Sci U S A* 101:5123–5128. [CrossRef](#) [Medline](#)
- Vialou V, Bagot RC, Cahill ME, Ferguson D, Robison AJ, Dietz DM, Fallon B, Mazei-Robison M, Ku SM, Harrigan E, Winstanley CA, Joshi T, Feng J, Berton O, Nestler EJ (2014) Prefrontal cortical circuit for depression- and anxiety-related behaviors mediated by cholecystinin: role of  $\Delta$ FosB. *J Neurosci* 34:3878–3887. [CrossRef](#) [Medline](#)
- Vialou V, Thibault M, Kaska S, Cooper S, Gajewski P, Eagle A, Mazei-Robison M, Nestler EJ, Robison AJ (2015) Differential induction of FosB isoforms throughout the brain by fluoxetine and chronic stress. *Neuropharmacology* 99:28–37. [CrossRef](#) [Medline](#)
- Vicini S, Wang JF, Li JH, Zhu WJ, Wang YH, Luo JH, Wolfe BB, Grayson DR (1998) Functional and pharmacological differences between recombinant N-methyl-D-aspartate receptors. *J Neurophysiol* 79:555–566. [CrossRef](#) [Medline](#)
- Wada Y, Shiraishi J, Nakamura M, Hasegawa H (1995) Prolonged but not acute fluoxetine administration produces its inhibitory effect on hippocampal seizures in rats. *Psychopharmacology* 118:305–309. [CrossRef](#)
- Wilson MA, Tonegawa S (1997) Synaptic plasticity, place cells and spatial memory: study with second generation knockouts. *Trends Neurosci* 20:102–106. [Medline](#)
- Yan Q-S, Jobe PC, Dailey JW (1994) Evidence that a serotonergic mechanism is involved in the anticonvulsant effect of fluoxetine in genetically epilepsy-prone rats. *Eur J Pharmacol* 252:105–112. [Medline](#)
- You JC, Muralidharan K, Park JW, Petrof I, Pyfer MS, Corbett BF, LaFrancois JJ, Zheng Y, Zhang X, Mohila CA, Yoshor D, Rissman RA, Nestler EJ, Scharfman HE, Chin J (2017) Epigenetic suppression of hippocampal calbindin-D28k by  $\Delta$ FosB drives seizure-related cognitive deficits. *Nat Med* 23:1377. [CrossRef](#) [Medline](#)
- Zhang W, Linden DJ (2003) The other side of the engram: experience-driven changes in neuronal intrinsic excitability. *Nat Rev Neurosci* 4:885. [CrossRef](#) [Medline](#)
- Ziv NE, Smith SJ (1996) Evidence for a role of dendritic filopodia in synaptogenesis and spine formation. *Neuron* 17:91–102. [Medline](#)